RECENT SPACE DEBRIS RELATED ACTIVITIES AT THE SLR STATION GRAZ

Michael A. Steindorfer[(1)], Georg Kirchner[(1)], Franz Koidl[(1)], Peiyuan Wang[(1)], Daniel Kucharski[(2)]

[(1)] Space Research Institute, Austrian Academy of Sciences, Lustbühelstraße 46, A-8042 Graz, Austria, Email: michael.steindorfer@oeaw.ac.at
[(2)] Space Environment Research Centre, SERC, Mount Stromlo Observatory, Canberra, Australia

ABSTRACT

The satellite laser ranging station Graz is currently involved in many different space debris related projects and experiments. Besides the presentation of technological improvements this paper will focus on attitude determination and observation strategies. A new space debris laser is mounted directly on the telescope avoiding any Coudé path providing easier alignment and usability. Within the second phase of the expert coordination center an approach was developed to validate and qualify passive-only SLR stations. High resolution light curves are recorded utilizing single photon avalanche detectors with up to 10 µs temporal resolution. A stare and chase approach allows pointing determination, orbit determination and space debris laser ranging within a single pass.

1 INTRODUCTION

Within this paper an update on recent developments regarding space debris laser ranging at the Satellite Laser Ranging (SLR) station Graz is given.

2 LASER ON ASTRONOMY TELESCOPES

The SP-DART (Single Photon - Detection, Alignment and Reference Tool) concept, improving an astronomy telescope to a fully functional SLR station, was presented by Graz SLR station in the year 2015 [1]. Two compact lasers (532 nm, 15µJ@2kHz and 1064nm, 30µJ@2kHz) including beam expansion optics were directly mounted on an astronomical telescope. Such a setup has the big advantage that any Coudé path (a number of mirrors reflecting the laser from the lab to the telescope) can be avoided. Besides lower costs alignment is much easier and pointing is more exact. A compact control unit handles the interaction with two detectors and handles event timing, range gate generation, GNSS time & clock reference and meteorological data. The system was successfully installed at several different SLR stations and astronomy telescopes and can also be used as a reference tool. Within the development of the new ESA SLR station located on Tenerife this concept will be applied for mounting a picosecond laser on the telescope [2].

As the development of more compact and powerful lasers continues this concept was now applied to space debris lasers. The laser head of a new space debis laser (532nm/80mJ or 1064nm/160mJ@200Hz) was directly mounted on the telescope of Graz SLR station (Fig. 1). In the base of the telescope the cooling unit and the power supply were installed. Cooling liquid and power supply cables were guided through the altitude and azimuth axis of the telescope.

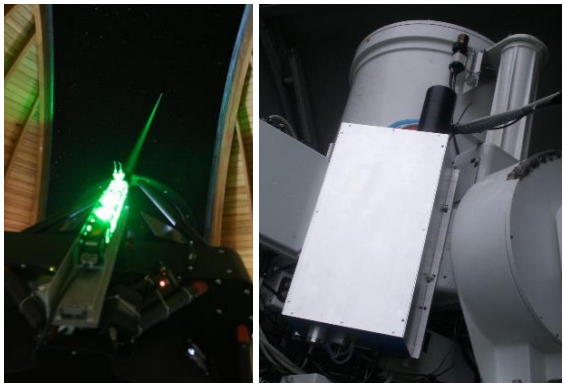

Figure 1. SP-DART mounted in Sandl, Austria (left) and the new space debris laser head mounted on the Graz SLR telescope (right).

The new setup was successfully tested in 15 space debris sessions collecting more than 200 passes of various debris targets. As an example, the range residuals to a SL-16 R/B (NORAD ID: 22566) having a time bias of -144ms and a range bias of 227m (Fig. 2) and an ARIANE 40 R/B (NORAD ID: 22830) with a time bias of -138ms and a range bias of 10 m are shown (Fig. 3) The x-axis shows the seconds of day 278/2018, the y-axis the observed-minus-calculated residuals [m].

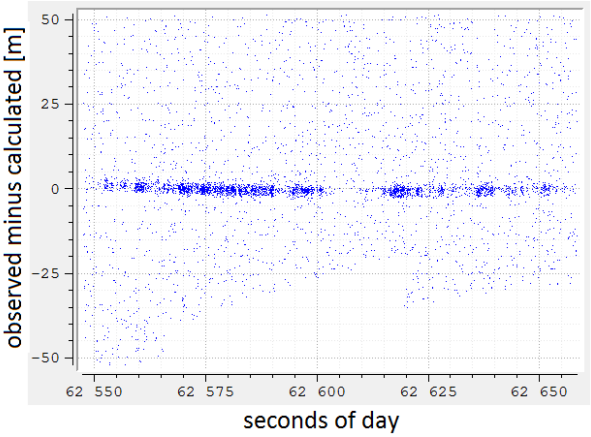

Figure 2. Space debris results to a SL-16 R/B (NORAD ID: 22566)

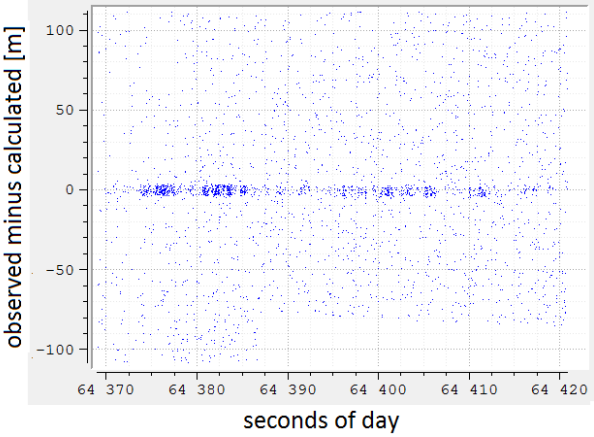

Figure 3. Space debris results to an ARIANE 40 R/B (NORAD ID: 22830).

Space debris ranging to Envisat (NORAD ID: 27386) clearly shows that the signal is composed of two parts. At the beginning of the pass until the second 63320 the individual retro-reflectors are visible. Afterwards the reflections of the retro-reflectors disappear and only the diffusely reflected photons appear having residuals of up to 9m, highlighting the shape of Envisat (Fig. 4).

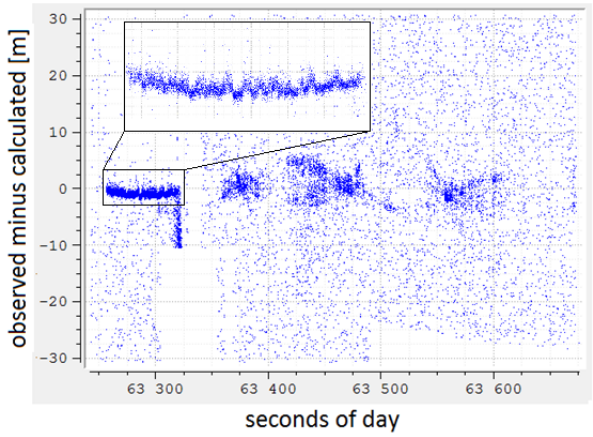

Figure 4. Space debris results to Envisat (NORAD ID: 27386).

3 ALCANTARA

Fine detailed structures were found within kHz SLR data to Galileo 103 (Fig. 5). Calculating the laser beam incident angle geometry on the panel (including yaw steering) it was found that during the pass the station appeared under an elevation of approx. 11.38° and an azimuth angle of 90° (as seen from the panel reference frame, including yaw steering. At these conditions the individual columns of the retro-reflector array appear at different distances and hence lead to a range offset within the data. From a histogram analysis (Fig. 6) the distances of these columns were derived and together with the retro-reflector arrangement the incident angle was calculated. The calculated incident angle perfectly matches the predicted one to be 11.37°.

This method provides a perfect way to validate the attitude of Galileo satellites and is only possible by analyzing the fine details of mm-accuracy kHz SLR data. It could also be applied to attitude analysis of e.g. defunct satellites with retroreflector panels. With known panel geometry SLR patterns could be simulated and compared to the actual measurements.

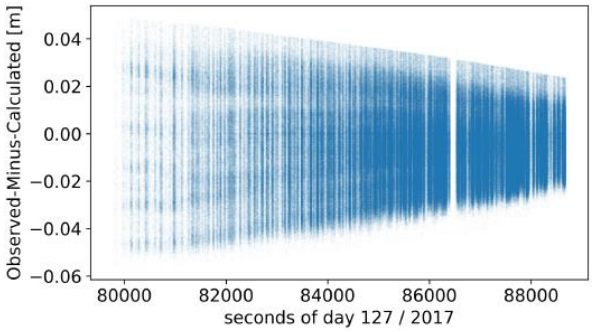

Figure 5. Range measurements to Galileo 103 revealed fine structures within the kHz SLR data corresponding to the individual columns of retro-reflectors. From the range offsets the incident angle was derived (11.37°)

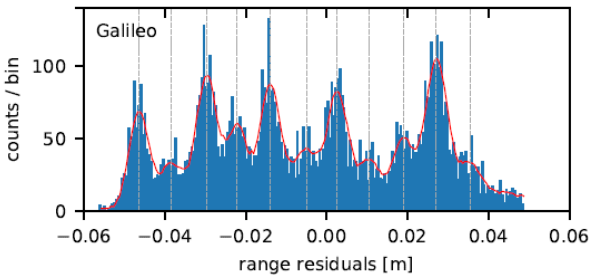

Figure 6. Histogram analysis through the dataset between second 79920 and 80300.

4 DAYLIGHT SPACE DEBRIS DETECTION

Debris laser ranging is currently limited to terminator periods, which is the time after sunset or before sunrise where satellites are sunlit while on Earth it is already sufficiently dark. Due to the low accuracy of two line element (TLE) predictions it is necessary to make targets optically visible. To improve the amount of data gathered by space debris laser ranging stations it is hence necessary to extend the observation times to daylight.

The number of photons arriving at a detector from a star can be expressed by using the spectral flux density S given in Jansky which is connected to the stellar magnitude mag via the following formula

$$S[\mu J] = 10^{\frac{23.9-mag}{2.5}} \quad (1)$$

1 Jansky corresponds to the unit of 10^{-26} W / (m^2 Hz). For a given wavelength of light and a given telescope aperture the corresponding power in Watts can be calculated. The number of photons per second is the given knowing the energy of the single photon.

The daylight brightness of the sky was estimated to be approx. 3 mag/arcsec^2. The field of view of one camera sensor pixel with 3.75µm pixel on a 5m focal length telescope is calculated to be 0.024 arcsec^2. Assuming that the star is covering 100 pixels on the detector, the total field of view corresponds to 2.4 arcsec^2. The brightness difference of two different fluxes is given by

$$mag = -2.5 * \log(\frac{F_1}{F_2}) \quad (1)$$

The two fluxes to be compared are the sky flux in one arcsec^2 and the flux of the sky area covered by the star. For the values given above a difference of -0.95 magnitudes results in a sky brightness of 2.05, which adds up to the stellar brightness. In the following the percentage P of starlight with respect to the total light is calculated

$$C = \frac{I_{star}}{I_{star}+I_{sky}} \quad (1)$$

using the number of photons arriving of the sky I_{sky} and the star I_{star} (Fig. 7).

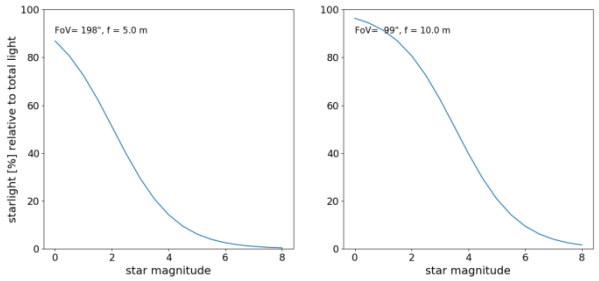

Figure 7. Percentage of starlight arriving at the detector with respect to the total light (including sky background).

The calculations show that with the parameters of our optical telescope (f=5.0m, left graph) it should be possible to observe star magnitudes of up to magnitude 7 or 8 during broad daylight. This assumes that approx. 1% of starlight can be separated via image analysis and software tools. Increasing the focal length of the telescope, decreasing the pixel size or reducing the number of pixels of the star on the detector could further improve the results. The first two parameters, however, come at a cost of decreased field of view which is not beneficial during space debris observations, as the TLE-based predictions will have a significant offset. The field of view of the camera itself should not influence the limiting magnitude, as the pixel size of the detector is important.

The following image shows a composition of different stars on an ASI 120 camera (pixel size: 3.75µm, detector size: 4.8mm x 3.2mm). Stars of up to a magnitude of 8.4 were visible (Fig. 8)

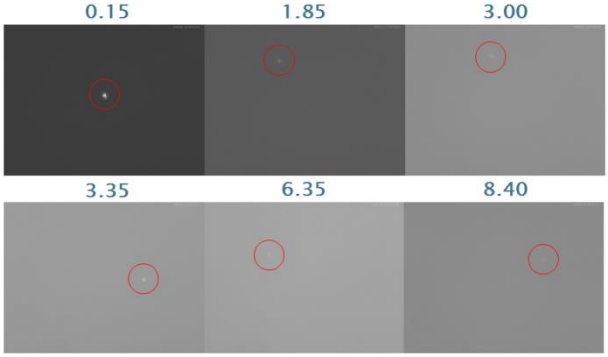

Figure 8. Daylight observations of stars of various magnitudes with an ASI 120 camera (pixel size: 3.75µm, detector size: 4.8mm x 3.2mm)

The same results were achieved with an ASI 1600 camera (pixel size: 3.75, detector size: 17.7 x 13.4 mm). In the image below (Fig. 9) a star of magnitude 5.1 was clearly visible.

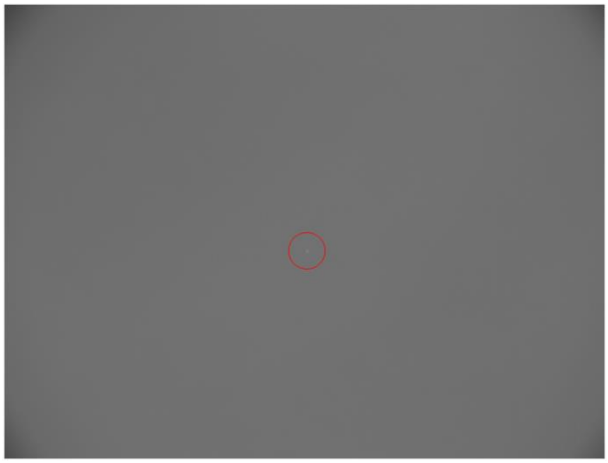

Figure 9. Daylight observation of a star with magnitude 5.1 with an ASI 1600 camera (pixel size: 3.75µm, detector size: 17.7 x 13.4 mm)

The ASI1600 and a full frame DSLR (digital single-lens reflex) camera were then used to track various space debris objects during daylight. The following Tab. 1 summarizes the results, including the NORAD ID, a short description and the NORAD ID and the radar cross section (RCS).

Table 1. Summary of visually observed space debris target during daylight, including NORAD ID, description and radar cross section (RCS) and distance d [km]

NORAD	Description	RCS [m^2]	d [km]
2802	SL-8 R/B	4.6	707-800
5118	SL-3 R/B	6.9	498-564
5730	SL-8 R/B	5.7	386-1394
12465	SL-3 R/B	5.7	507-554
14820	SL-14 R/B	3.8	612-638
15772	SL-12 R/B(2)	14.4	801-855
16111	SL-3 R/B	5.9	388-409
19120	SL-16 R/B	10.7	820-850
20625	SL-16 R/B	14.0	839-862
22220	SL-16 R/B	15.2	837-853
22830	ARI 40 R/B	9.8	786-803
23343	SL-16 R/B	8.9	641-652
24298	SL-16 R/B	8.8	549-867
25861	SL-16 R/B	13.5	629-653

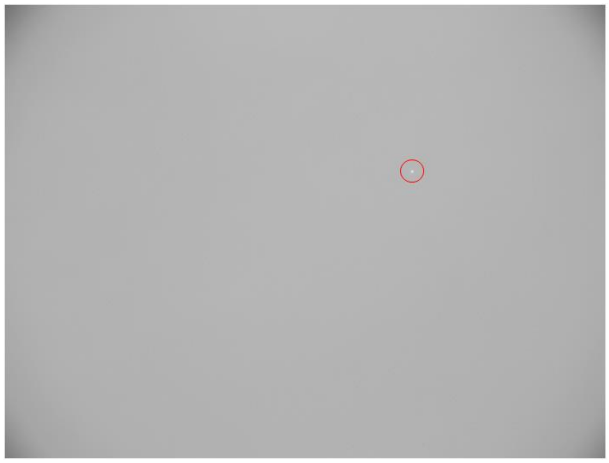

Figure 10. Daylight observation of the SL-12 rocket body (NORAD ID: 15772) with an ASI 1600 camera (pixel size: 3.75µm, detector size: 17.7 x 13.4 mm).

As preparation for actual space debris ranging during daylight a program was written to extract time bias information from the image. The space debris object will then be observed visually with a first telescope and the time bias forwarded the to the SLR station. This will decrease the area on the sky which needs to be searched to hit the debris with the laser significantly.

5 STARE AND CHASE

Within the framework of ESA project 4000112734/14/D/SR 'Space debris stare and chase', SLR station Graz successfully implemented the "Stare & Chase" approach ranging to space debris targets without a-priori knowledge of any orbital information [3]. A low cost camera system with a field of view of approx. 10° "stares" into an arbitrary direction of the sky and records the stellar background up to magnitude 9. From the position of stars the pointing direction of the camera is derived. If sunlit space debris or a satellite passes through the field of view (Fig. 11), the celestial coordinate, referenced to the stellar background, are determined. Using only this pointing information – without a-priori orbital information – a CPF orbit is calculated and immediately used to track ("chase") the target and to perform laser-based distance measurements (Fig. 12).

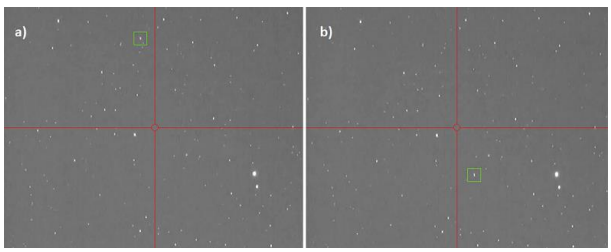

Figure 11. Haiyang 2A passes through the field of view of the Stare & Chase camera. To determine the pointing direction of the image center a plate solving algorithm

is used while recording the stellar background. The current X/Y position of the satellite (highlighted with a green rectangle) is transformed to equatorial coordinates.

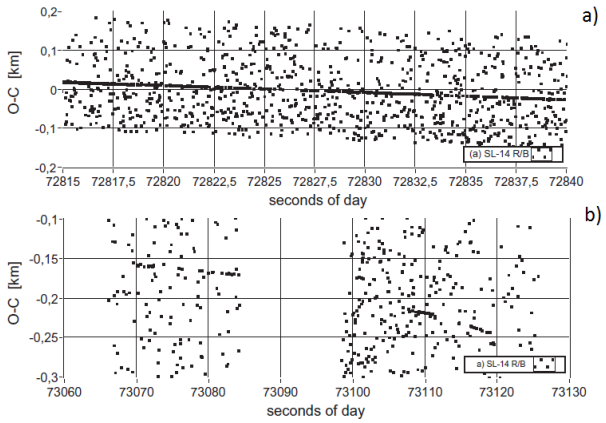

Figure 12. Space debris ranging observed-minus calculated residuals (O-C) of TLE-based tracking (a) compared to "stare and chase"-based tracking (b) to a SL-16 rocket body (NORAD ID: 33505)

6 ENVISAT SPIN RATE DETERMINATION

The spin parameters of ENVISAT can be measured by Satellite Laser Ranging and photometric systems. The observation data collected by multiple systems is analysed in order to monitor the development of the satellite's spin dynamics since the end of the mission (April 8, 2012). The apparent spin rate from light curves is determined with the Phase Dispersion Minimization method which finds the periodic variation in the time series by minimizing the dispersion of the folded data set. The meter-scale oscillations of the laser range measurements to the satellite's retro-reflector array indicate the rotational period of the spacecraft. The observed spin period is corrected for the apparent rotation that adds up to the measurements as a result of the view angle change during the satellite pass over the ground station. The resulting inertial spin trend of ENVISAT is presented on Fig. 13 (212 passes, RMS 3%).

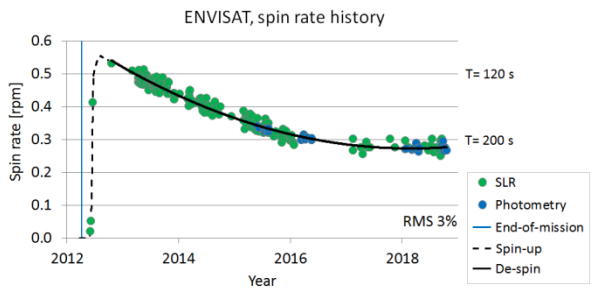

Figure 13. ENVISAT spin trend, June 2012 - Oct 2018.

The initial spin-up of the satellite occurred during a time span of nearly two months and produced an estimated spin rate of 0.547 rpm (spin period of 110 s). The continuous loss of the rotational energy is observed from August 2012 until 2017 and is caused by the interaction of the satellite with the Earth's magnetic field that dissipates the spin energy through the flow of eddy currents in the conductive elements of the body. The spin observations collected over the last two years (2017-2018) suggest that ENVISAT entered a flat-spin trend where the forces acting on the satellite produce an overall zero-torque output that stabilizes the spin period of the body at T=217 s (RMS 9.9 s). Further analysis will be conducted in order to model the forces causing the flat-spin phenomenon and the possible duration of this dynamical stage.

7 SUMMARY AND CONCLUSION

In this paper we present recent developments of space debris related act ivies at Graz SLR station.

Daylight observation of stars and space debris rocket bodies showed promising results providing a visibility down to magnitude 8. Theoretical calculations analyzing the contrast of stars of different magnitudes relative to the daylight sky gave similar results. It was found that in the last year the spin period of ENVISAT stabilized to approximately 217s. The "Stare & Chase" approach allowed ranging to space debris part without a-priori knowledge of any predictions. The SP-DART concept was successfully extended a space debris laser which was mounted directly on our telescope significantly reducing alignment effort and providing easier setup.

8 REFERENCES

1. Kirchner G., Steindorfer M.A., Koidl F, *et al.* (2015) SP-DART: Single-Photon Detection, Alignment and Reference Tool. *2015 ILRS Technical Workshop*. 1–7.

2. Kloth A., Steinborn J., Munder J., *et al. (2018)* Towards Turnkey SLR Systems: New ESA Laser Ranging Station (ELRS). *21st Insternational Workshop on Laser Ranging*.

3. Steindorfer M.A., Kirchner G., Koidl F., *et al.* Stare and chase of space debris targets using real-time derived pointing data. *Adv. Sp. Res.* **60**, 1201–1209.